

Properties of a Fermi liquid at the superfluid transition in the crossover region between BCS superconductivity and Bose-Einstein condensation

R. Haussmann

Sektion Physik der Ludwig-Maximilians-Universität München, Theresienstrasse 37, D-80333 München, Germany

(Received 20 September 1993)

The self-consistent equations, which have been derived recently as a microscopic model for the crossover between BCS superconductivity and Bose-Einstein condensation in a three-dimensional interacting Fermi system [R. Haussmann, *Z. Phys. B* **91**, 291 (1993)], are solved numerically by repeated Fourier transformation. We find a superfluid transition temperature T_c which increases monotonically with increasing attractive coupling strength. Furthermore, we determine the chemical potential μ , the fermion distribution function $n(k)$, and the complex effective mass $2m^*$ of the fermion pairs at $T=T_c$. The bound fermion pairs cause a power-law tail $\sim k^{-4}$ in $n(k)$ for large k and behave as short-living quasiparticles in the crossover region, which is indicated by a large imaginary part of $2m^*$.

I. INTRODUCTION

Recently we have proposed a microscopic theory¹ for a three-dimensional liquid of fermions with an instantaneous short-range interaction of variable strength, which allows the formation of bound fermion pairs and a superfluid phase transition under certain conditions. This theory is given by two sets of self-consistent equations, which we have derived within the framework of many-particle quantum-field theory with temperature-dependent Green's functions.^{2,3}

In our previous paper¹ we have discussed the self-consistent equations in the two limiting cases of weak and strong attractive interaction forces between the fermions. In these cases the problem can be treated analytically by performing some controlled approximations. Thus in the weak-coupling limit we have found a normal Fermi liquid which becomes superfluid below a certain critical temperature T_c according to the Bardeen-Cooper-Schrieffer (BCS) theory. In the strong-coupling limit the fermions are bound into pairs by the strong attractive interaction forces, if the temperature T is well below the dissociation temperature $T_{\text{diss}} \approx \epsilon_b/k_B$, which is determined by the binding energy ϵ_b of the pairs. The bound pairs form an interacting gas of bosons, which becomes superfluid below T_c via the Bose-Einstein condensation, while the strength of interaction between the bosons tends to zero in the ultimate strong-coupling limit.

However, in the crossover region between weak and strong coupling the system is a mixture of free fermions and bound fermion pairs, which behave as rather short-living fermionic and bosonic quasiparticles, respectively, because a pair will decay into two free fermions and two free fermions will recombine into one pair. These decay and recombination processes imply rather complicated spectral functions of the quasiparticles. Therefore, the self-consistency of the equations is essential so that no analytically tractable approximations can be made but instead the complete self-consistent equations must be solved numerically. Thus, in this paper we present a nu-

merical treatment of our self-consistent equations. This will be done by iteration of the equations and repeated Fourier transformation of the Green's and vertex functions until convergence is achieved. The numerical Fourier transformation is highly nontrivial because the functions have rather subtle singularities. In Sec. II and in the Appendix we briefly describe how we have solved this problem with comparatively modest numerical effort.

In Sec. III we present the result of our self-consistent theory. We concentrate our numerical analysis on the superfluid transition and calculate T_c and the chemical potential μ_c as functions of the interaction strength from weak to strong coupling. At T_c we determine some other quantities, which reflect the crossover scenario from BCS superconductivity to Bose-Einstein condensation. We calculate the fermion occupation number $n(k)$ and show that the bound pairs cause a power-law tail $\sim k^{-4}$ for large k . Of special interest are the kinematical properties of the bound fermion pairs, which are represented by the effective boson mass $2m^*$ defined in a similar manner as in Ref. 4. We find that $2m^*$ is nearly twice the fermion mass in the strong-coupling limit, while it becomes complex in the intermediate and weak-coupling range due to the existence of unbound single fermions.

The superfluid transition temperature T_c as a function of the coupling strength was calculated by Nozières and Schmitt-Rink⁵ in 1984. They considered a three-dimensional gas of fermions with an attractive two-particle interaction and used an approximation scheme, which is equivalent to a ladder approximation² with free-fermion Green's functions. As a result they obtained a T_c , which interpolates between the two limiting cases, the BCS theory, and the Bose-Einstein condensation. A second approach is due to Drechsler and Zwerger.⁶ Starting from a functional integral representation of the interacting fermions Drechsler and Zwerger introduced the order parameter $\Delta(\mathbf{x}, \tau)$ via a Hubbard-Stratonovich transformation. Integrating out the fermion degrees of freedom and expanding in powers of $\Delta(\mathbf{x}, \tau)$ they obtained a Ginzburg-Landau theory. Though this theory

was originally designed for a two-dimensional system,⁶ it has been extended recently to three dimensions.⁷ Sá de Melo, Randeria, and Engelbrecht⁸ have proposed a time-dependent Ginzburg-Landau theory, and in close analogy to Ref. 5 they determined the superfluid transition temperature T_c , which exhibits a small maximum in the crossover region.

All these previous theories are based on an approximation scheme which uses *free-fermion* Green's functions to take the fermionic degrees of freedom into account, while the bosonic properties lead to the superfluid transition. In the two limiting cases of weak and strong coupling this approximation leads to correct results. However, in the crossover region this approximation is *invalid* because the fermionic quasiparticles are far from being free particles. Therefore in an improved theory the fermion Green's function must be determined *self-consistently*. This will lead to qualitative new results as we will show in this paper. In the strong-coupling limit the theories of Refs. 4–6 and 8 lead to a Bose gas of fermion pairs, while missing an interaction between the *noncondensed* bosons. Within our self-consistent theory we have shown recently¹ by performing a next-to-leading-order approximation that in the strong-coupling limit there exists a small repulsive interaction between the bosons $a_B = 2a_F$ due to the Pauli exclusion principle. (The result $a_B = 2a_F$ has been obtained independently in Refs. 7 and 8 from the interaction between the *condensed* bosons.) This interaction causes an increase of the effective boson mass and a decrease of T_c as it is expected from the theory of the weakly interacting Bose gas (see Sec. 28 of Ref. 2). From this observation we have argued¹ that T_c as a function of the coupling strength should *increase monotonically* from weak to strong coupling. This is true at least asymptotically in the strong-coupling limit, where nearly all fermions are bound to pairs. In this paper we will show by solving the complete self-consistent equations numerically that for a three-dimensional system T_c is indeed a monotonic function in the whole coupling range, and that there exists no maximum of T_c in the crossover region.

II. THE SELF-CONSISTENT EQUATIONS AND THEIR NUMERICAL TREATMENT

Above T_c the normal-fluid Fermi liquid is described by the scalar fermion Green's function $\mathcal{G}(\mathbf{k}, \omega_n)$, which represents the fermionic properties, and the vertex function $\Gamma(\mathbf{K}, \Omega_n)$, which is a generalized scattering amplitude (T matrix) and which represents the bosonic properties of the system. For $T > T_c$ the self-consistent equations are given by¹ the Dyson equations

$$\mathcal{G}(\mathbf{k}, \omega_n) = \frac{1}{-i\hbar\omega_n + (\hbar^2\mathbf{k}^2/2m - \mu) - \Sigma(\mathbf{k}, \omega_n)}, \quad (1)$$

$$\Sigma(\mathbf{x}, \tau) = \mathcal{G}(-\mathbf{x}, -\tau) \cdot \Gamma(\mathbf{x}, \tau) \quad (2)$$

and the Bethe-Salpeter equations

$$\Gamma(\mathbf{K}, \Omega_n) = \frac{4\pi\hbar^2}{m} \frac{1}{a_F^{-1} + M(\mathbf{K}, \Omega_n)}, \quad (3)$$

$$M(\mathbf{x}, \tau) = \frac{4\pi\hbar^2}{m} \left[[\mathcal{G}(\mathbf{x}, \tau)]^2 - c \cdot \delta(\mathbf{x}) \cdot \hbar \sum_n \delta(\tau - n\hbar\beta) \right], \quad (4)$$

where c is an infinite renormalization constant, which effects dimensional regularization. The approximation scheme, which we have used for deriving Eqs. (1)–(4) is known as the Brueckner-Hartree-Fock method in nuclear physics.⁹ The functions with different arguments are related to each other by Fourier transformation

$$\mathcal{G}(\mathbf{x}, \tau) = \int \frac{d^3k}{(2\pi)^3} \frac{1}{\beta} \sum_{\omega_n} \exp[i(\mathbf{k}\mathbf{x} - \omega_n\tau)] \cdot \mathcal{G}(\mathbf{k}, \omega_n), \quad (5)$$

$$\Gamma(\mathbf{x}, \tau) = \int \frac{d^3K}{(2\pi)^3} \frac{1}{\beta} \sum_{\Omega_n} \exp[i(\mathbf{K}\mathbf{x} - \Omega_n\tau)] \cdot \Gamma(\mathbf{K}, \Omega_n). \quad (6)$$

$\Sigma(\mathbf{k}, \omega_n)$ and $M(\mathbf{K}, \Omega_n)$ are transformed analogously. Here τ is the imaginary time (temperature parameter) varying in the interval $0 < \tau < \hbar\beta = \hbar/k_B T$, and ω_n and Ω_n are the fermionic and the bosonic Matsubara frequencies, respectively.^{2,3} The superfluid transition at $T = T_c$ is determined by the Thouless criterion¹⁰

$$[\Gamma(\mathbf{K}=\mathbf{0}, \Omega_n=0)]^{-1} = 0, \quad (7)$$

which means that the vertex function $\Gamma(\mathbf{K}, \Omega_n)$ has a pole at zero frequency and zero momentum.

Once we are able to perform the Fourier transformations, we can solve the self-consistent equations iteratively. Starting with the free-fermion Green's function

$$\mathcal{G}_0(\mathbf{k}, \omega_n) = 1/[-i\hbar\omega_n + \hbar^2\mathbf{k}^2/2m - \mu], \quad (8)$$

we obtain from (4) and (3) the vertex function $\Gamma(\mathbf{K}, \Omega_n)$ and then from (2) and (1) the fermion Green's function $\mathcal{G}(\mathbf{k}, \omega_n)$ in first order. This iteration procedure is repeated successively to obtain Γ and \mathcal{G} in higher orders until convergence is achieved.

Obviously the success of our method depends on the realization of an efficient and precise numerical Fourier transformation suitable for \mathcal{G} and Γ . From Eqs. (1) and (3) one can see that $\mathcal{G}(\mathbf{k}, \omega_n)$ and $\Gamma(\mathbf{K}, \Omega_n)$ decrease rather slowly for large (\mathbf{k}, ω_n) and large (\mathbf{K}, Ω_n) , respectively. This implies a rather subtle singular behavior of the real-space functions $\mathcal{G}(\mathbf{x}, \tau)$ and $\Gamma(\mathbf{x}, \tau)$ for $(\mathbf{x}, \tau) \rightarrow (\mathbf{0}, 0)$. The singular behavior can be weakened partially by subtracting the “free” functions \mathcal{G}_0 and Γ_0 , which are known analytically so that only the differences $\Delta\mathcal{G} = \mathcal{G} - \mathcal{G}_0$ and $\Delta\Gamma = \Gamma - \Gamma_0$ must be transformed numerically. On the other hand the nontrivial physical properties of the fermion system are included in the functions \mathcal{G} and Γ at intermediate values of their variables. Therefore we need a Fourier-transformation procedure, which resolves the functions well at *small*, *intermediate*, and *large* scales of the variables (\mathbf{k}, ω_n) , (\mathbf{K}, Ω_n) , and (\mathbf{x}, τ) , respectively. This means we need a resolution on a *logarithmic* scale of the variables. In the Appendix we describe the Fourier

transformation procedure, which we have constructed for solving the equations and for calculating the quantities in Sec. III and which is appropriate to transform functions like \mathcal{G} and Γ .

III. NUMERICAL RESULTS AND DISCUSSIONS

The state of the fermion system is determined by three parameters, the temperature T , the chemical potential μ , which is related to the fermion density n_F , and the strength of the attractive interaction between the fermions, which is determined by the inverse s -wave scattering length a_F^{-1} . This can be seen in the self-consistent equations (1)–(4). While μ and a_F^{-1} are contained explicitly in (1) and (3), respectively, the temperature T is included via the Matsubara frequencies $\omega_n = (2n+1)\pi k_B T/\hbar$ and $\Omega_n = 2n\pi k_B T/\hbar$ with $n \in \mathbb{Z}$. Since the interaction between the fermions is assumed to be of zero range, one can show easily that the self-consistent equations are invariant under the scaling transformation $a_F \rightarrow \kappa a_F$, $T \rightarrow \kappa^{-2} T$, $\mu \rightarrow \kappa^{-2} \mu$. This scale invariance is very convenient for investigating the system at *constant* fermion density $n_F = -2 \cdot \mathcal{G}(\mathbf{x}=\mathbf{0}, \tau=-0)$ because the scaling transformation can be used to normalize the parameters with respect to n_F . Since the fermion density is transformed by $n_F \rightarrow \kappa^{-3} n_F$ we introduce the dimensionless quantities

$$T/T_{c,BE}, \quad \mu/\epsilon_F, \quad v = 1/k_F a_F, \quad (9)$$

which are scale invariant and normalized with respect to n_F because $k_F = (3\pi^2 n_F)^{1/3}$ is the Fermi wave number, $\epsilon_F = \hbar^2 k_F^2/2m$ is the Fermi energy of an ideal Fermi gas, and $T_{c,BE} = [2\pi\hbar^2/2mk_B][n_F/2]/\zeta(3/2)^{2/3}$ is the Bose-Einstein–condensation temperature of an ideal Bose gas of $n_F/2$ bosons (fermion pairs) per volume with mass $2m$.

A. Superfluid transition temperature T_c and chemical potential μ_c

At the superfluid transition T_c and μ_c can be determined uniquely by the Thouless criterion (7) if a_F^{-1} and n_F are known. Using the scale invariance and Eqs. (9) we obtain T_c and μ_c from our numerical calculations in units of $T_{c,BE}$ and ϵ_F , respectively, as functions of the invariant coupling strength v . In this way the fermion density n_F is effectively fixed. In Fig. 1 we present our numerical result for $T_c(v)$ as full line. First of all we see that $T_c(v)$ is a continuous function of v , which means that the crossover from BCS superconductivity to Bose-Einstein condensation is *continuous*, which agrees with all previous theories. In the weak-coupling limit $v \rightarrow -\infty$ the BCS-transition temperature (dashed line on the left) is approached asymptotically,

$$T_c(v) \rightarrow (e^{\gamma_E}/\pi)(8/e^2)(\epsilon_F/k_B) \exp(v\pi/2), \quad (10)$$

which tends to zero exponentially. On the other hand, in the strong-coupling limit $v \rightarrow +\infty$ the Bose-Einstein–condensation temperature $T_{c,BE}$ is approached asymptotically from below. In our preceding paper¹ we have calculated the leading correction due to the repulsive interaction between the composite bosons, which is

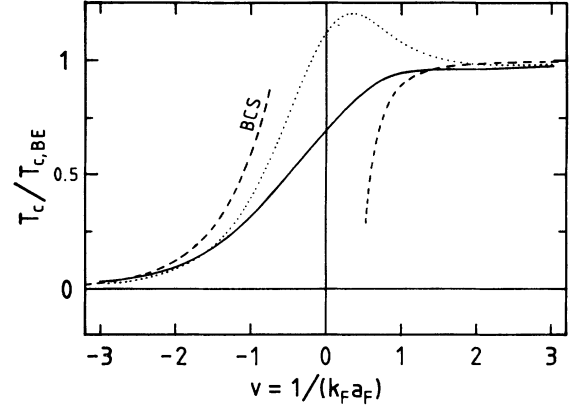


FIG. 1. The superfluid transition temperature $T_c(v)$ as a function of the dimensionless coupling strength $v = 1/k_F a_F$ for constant fermion density n_F . The full line represents the numerical result of our self-consistent theory. The dotted line is obtained by neglecting self-consistency and is similar to the results of the previous theories (Refs. 5 and 8). The left-hand dashed line corresponds to the BCS theory, (10). The right-hand dashed line corresponds to our first-order asymptotic formula (11) including the interaction between the fermion pairs.

represented by the right dashed line in Fig. 1 and given by the asymptotic formula

$$T_c(v) \rightarrow T_{c,BE} [1 - (3\pi)^{-1} v^{-3}]. \quad (11)$$

We have found that our numerical calculations work quite well in the crossover region $-1 \lesssim v \lesssim +1$ and yield $T_c(v)$ with a relative accuracy of about 1%. In the limiting cases the numerical inaccuracies are somewhat larger. For strong coupling the additional inaccuracies are mainly due to an uncertainty in the fermion density $n_F = -2 \cdot \mathcal{G}(\mathbf{x}=\mathbf{0}, \tau=-0)$ because for $v \gtrsim +1$ nearly all fermions are bound to pairs and the leading contribution to n_F originates from the boson density $n_b = -[8\pi\epsilon_F^2 a_F^3]^{-1} \cdot \Gamma(\mathbf{x}=\mathbf{0}, \tau=-0)$, which is included only indirectly in (1) via the self-energy $\Sigma(\mathbf{k}, \omega_n)$ (see Ref. 1). This fact is the reason why the full line in Fig. 1 does not approach the asymptotic dashed line quite well for $v \rightarrow +\infty$. On the other hand for weak coupling $v \lesssim -1$ a more and more well-defined Fermi surface occurs in \mathbf{k} space, which leads nearly to a discontinuity in the fermion occupation number $n(k)$ at $k \approx k_F$ and thus to oscillations of $\mathcal{G}(\mathbf{x}, \tau)$ in real space. While we have resolved the Fermi surface quite well, the oscillations have not been treated appropriately, so that additional numerical errors occur in our results for weak coupling $v \lesssim -1$.

In Fig. 1 one clearly sees that the full line increases monotonically with increasing interaction strength v . This is the numerical evidence of the statement we have given earlier¹ based on the observation that asymptotically in the strong-coupling limit $v \rightarrow +\infty$ the transition temperature T_c increases monotonically and converges to $T_{c,BE}$ from below (right-hand dashed line). For comparison we have determined $T_c(v)$ neglecting self-consistency, which is shown as dotted line in Fig. 1. To do this we have inserted the *free-fermion* Green's func-

tion (8) into (4) and (2) and then determined Γ and \mathcal{G} by (3)–(1). This approximation does not include the repulsive interaction between the pairs and is *equivalent* to the approximations of the previous theories.^{4–6,8} The dotted line in Fig. 1 clearly shows a maximum in the crossover region, which is a considerable effect. This result looks similar like that of Nozières and Schmitt-Rink⁵ and that of Sá de Melo, Randeria, and Engelbrecht.⁸ While Nozières and Schmitt-Rink have pointed out that the maximum is presumably an artifact of their approximations, we find that there is no maximum if and only if the interaction between the bound pairs is included. Recently Stintzing and Zwerger⁷ extended the Ginzburg-Landau theory including the interaction between the noncondensed fermion pairs by taking the $|\Psi|^4$ term into account and thus confirmed our results in the strong-coupling limit.

In Fig. 2 the chemical potential μ_c at the superfluid transition is shown in units of the Fermi energy $\epsilon_F = \hbar^2 k_F^2 / 2m$ as a function of the dimensionless coupling strength $v = 1/k_F a_F$. The full line represents our numerical result. In the weak-coupling limit $v \rightarrow -\infty$ we find $\mu_c \rightarrow \epsilon_F$ according to the BCS theory. Including the first-order correction due to a weak attractive interaction between the fermions, the chemical potential reads approximately²

$$\mu_c \approx \epsilon_F [1 + (4/3\pi)v^{-1}], \quad (12)$$

which is shown as the left dashed line in Fig. 2. The convergence of the full line to this dashed line is quite good. In the strong-coupling limit $v \rightarrow +\infty$ we have $\mu_c \rightarrow -\epsilon_b/2 = -\hbar^2/2ma_F^2$ or $\mu_c/\epsilon_F \rightarrow -v^{+2}$, which is represented by the right-hand dashed line in Fig. 2. This means that in the strong-coupling limit μ approximately becomes half of the binding energy ϵ_b of the pairs (compare with Ref. 4). The correction $\mu_B = 2\mu + \epsilon_b$ should be interpreted as bosonic chemical potential, which is always positive at T_c because of the *repulsive* interaction between the fermion pairs. One clearly sees that our numerical result of μ (full line) interpolates quite well be-

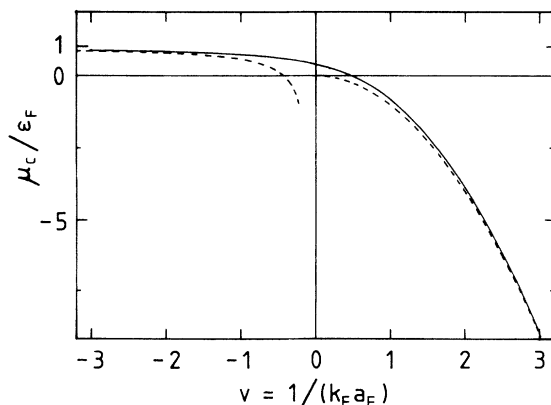


FIG. 2. The chemical potential μ_c at the superfluid transition as a function of the dimensionless coupling strength $v = 1/k_F a_F$. The full line represents our numerical result. The asymptotic result for the weakly interacting Fermi gas (12) is shown as left-hand dashed line. The right-hand dashed line corresponds to the binding energy of the fermion pairs divided by 2.

tween the two limiting cases (dashed lines). Numerical inaccuracies seem to be small here. The previous theories^{5,8} have found a chemical potential $\mu_c(v)$, which looks qualitatively similar like ours. However, there are differences in detail. While in our theory μ approaches $-\epsilon_b/2$ from above rather slowly for $v \rightarrow +\infty$, in the previous theories^{5,8} the convergence must be exponentially, as it is found also in our theory if self-consistency is neglected [the free-fermion Green's function (8) inserted into (4) and (2), see above] because there the interaction between the noncondensed bosons is neglected.

B. The fermion occupation number $n(k)$

Until now we have considered the *macroscopic* quantities T and μ , which determine the *thermodynamic* state of the system for a given coupling strength v . However, the functions $\mathcal{G}(\mathbf{k}, \omega_n)$ and $\Gamma(\mathbf{K}, \Omega_n)$ we have calculated numerically contain also information about the *microscopic* details of the system. A microscopic quantity of special interest is the fermion occupation number $n(k)$, which describes the distribution of the fermions among the single-particle states with momenta $\hbar\mathbf{k}$. Due to the attractive interaction part of the fermions are *free* and part of the fermions are *bound* to pairs. Thus $n(k)$ is non-trivial.

In Fig. 3 we show our numerical results of $n(k)$ for different values of the coupling strength v and for $T = T_c$. For $v = -1$ (and smaller values) $n(k)$ represents a degenerate weakly interacting Fermi gas. Most of the fermions are *free* fermions, which occupy the states of momenta $\hbar\mathbf{k}$ within the Fermi sphere $0 \leq k \lesssim k_F$ with a rather well-defined Fermi surface at $k \approx k_F$. The Fermi surface is smeared out by the finite temperature $T = T_c$ and by the weak interaction between the fermions. This form of $n(k)$ for $v \rightarrow -\infty$ is expected from the BCS theory. For $v = +2$ (and larger values) the fermionic system is nondegenerate because of $n(k) \ll 1$ for all values of k . Since the chemical potential is $\mu \ll -\epsilon_F$ nearly all fermions are bound into pairs. While for free fermions $n(k)$ would decay exponentially (for $T > 0$), the bound fermions are represented by the power-law decay $n(k) \sim k^{-4}$ for large

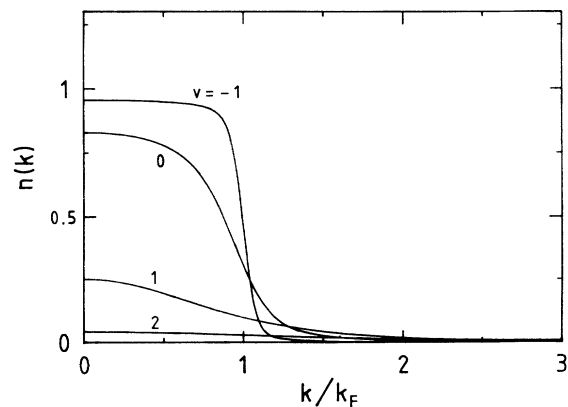


FIG. 3. The fermion occupation number $n(k)$ for various coupling strengths $v = -1, 0, +1, +2$ at $T = T_c$. While for weak coupling $v = -1$ the discontinuity of a Fermi surface at $k = k_F$ is indicated, $n(k)$ is small compared to 1 and given approximately by (13) for strong coupling $v = +2$.

k , which can be seen clearly as straight lines in the double logarithmic plot of Fig. 4. This result is caused by the relative motion of the fermions within the pairs and in the strong-coupling limit it can be interpreted as follows. For an effective zero range interaction the relative motion of two fermions in a pair is described by the wave function¹

$$\varphi_0(r) = [(2\pi a_F)^{1/2} r]^{-1} \exp(-r/a_F).$$

In momentum space it is

$$\varphi_0(k) = -(8\pi/a_F)^{1/2} [a_F^{-2} + k^2]^{-1},$$

which leads to $n(k) \sim |\varphi_0(k)|^2 \sim (1 + k^2 a_F^2)^{-2}$. Thus, in a more profound calculation¹ we have obtained

$$n(k) = 8\pi n_b a_F^3 / (1 + k^2 a_F^2)^2 \quad (13)$$

for $v \rightarrow +\infty$ up to leading order where $n_b = n_F/2$ is the density of pairs. An interaction with finite range r_0 would smoothen the singularity of $\varphi_0(r)$ at $r=0$. This would cause an exponential cutoff in $\varphi_0(k)$ and $n(k)$ for $k \gtrsim r_0^{-1}$. Therefore, in realistic cases the power law $\sim k^{-4}$ would be observed for not too large momenta $k \lesssim r_0^{-1}$. However, in our theory the range r_0 is assumed to be zero.

The power law $n(k) = S(k_F/k)^4$ for large k is not restricted to the strong-coupling limit, but it is observed for all coupling strengths v and even in the weak-coupling limit. This can be seen in Fig. 4. The amplitude S of the power-law depends monotonically on the coupling strength v . It is always positive and decreases with decreasing v . In the strong-coupling limit Eq. (13) yields $S = (4/3\pi)v$, which accords quite well with our numerical result for $v=2$ in Fig. 4. In conclusion we find that for an interaction of short-range r_0 bound fermion pairs are related to a power-law tail $\sim k^{-4}$ in the fermion occupation number $n(k)$ for momenta $\hbar k$ in the interval $\max(k_F, a_F^{-1}) \lesssim k \lesssim r_0^{-1}$. Nozières and Schmitt-Rink⁵ also calculated $n(k)$ and obtained a result, which looks qualitatively similar like our Fig. 3. However, they did not observe the *power-law* decay of the tails.

We have restricted our considerations to temperatures

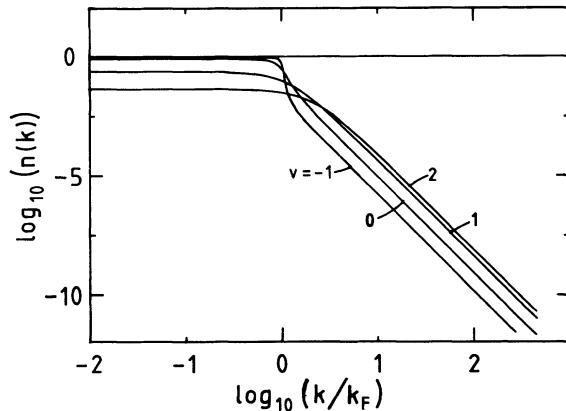


FIG. 4. Double-logarithmic plot of the fermion occupation number $n(k)$ vs k . For large k the power-law tails $n(k) \sim k^{-4}$ caused by the bound fermion pairs are clearly seen as straight lines for all couplings $v = -1, 0, +1, +2$.

$T = T_c(v)$. However, this restriction is not necessary. Since the superfluid transition at T_c is of *bosonic* nature and $n(k)$ is a *fermionic* quantity, we expect no qualitative change of the results of Figs. 3 and 4 if the temperature T is somewhat above or below T_c . This statement can be verified numerically and is confirmed by our observation that the structure of $n(k)$ is determined by the free and bound fermions, but not by the condensation of the pairs, which is related to the superfluid transition.

C. Kinematical behavior and the complex effective mass of the fermion pairs

Superfluidity is usually correlated with the existence of bosonic quasiparticles, which condense at low enough temperatures $T < T_c(v)$. In our fermionic system these bosonic quasiparticles are identified as fermion pairs. For strong coupling $v \gtrsim +1$ the fermion pairs are tightly bound and rather small and well-defined bosons. On the other hand, in the intermediate and weak-coupling regime $v \lesssim +1$ the fermion pairs are short-living quasiparticles, which interact with a sea of free fermions. Especially in the weak-coupling limit $v \ll -1$ where the BCS theory is valid, the pairs are rather large and penetrate each other because the diameter of the pairs is large compared to the mean distance between the fermions. Therefore, we expect an unusual kinematical behavior of the bound pairs for weak and intermediate couplings $v \lesssim +1$.

The microscopic properties of the bosonic quasiparticles are represented by the vertex function $\Gamma(\mathbf{K}, \Omega_n)$. In the strong-coupling limit $v \gg +1$ the vertex function is identified with the boson Green's function up to a constant factor, and for $T = T_c$ we have found¹

$$[\Gamma(\mathbf{K}, \Omega_n)]^{-1} = -[8\pi\epsilon_b^2 a_F^3]^{-1} Z^{-1} (-i\hbar\Omega_n + \hbar^2 \mathbf{K}^2 / 4m^*) \quad (14)$$

for sufficiently small Ω_n and \mathbf{K} , where up to first order

$$2m^* = 2m [1 + (3\pi)^{-1} v^{-3} + \dots] \quad (15)$$

is the effective boson mass and

$$Z = 1 + \pi^{-1} v^{-3} + \dots \quad (16)$$

is a renormalization factor. To investigate the kinematical properties of the bosons we must turn over to the linear-response formalism, which depends on the real time t or equivalently on the associated real *continuous* frequency z . To do this we introduce the corresponding susceptibility $\chi(\mathbf{K}, z)$, which is the analytical continuation of $\Gamma(\mathbf{K}, \Omega_n)$ where $i\Omega_n \rightarrow z$ is substituted. Thus from Eq. (14) we obtain

$$[\chi(\mathbf{K}, z)]^{-1} = d\hbar z - c\hbar^2 \mathbf{K}^2 / 2m \quad (17)$$

in the strong-coupling limit, where d and c are parameters related to $2m^*$ and Z . Below we will identify d and c as parameters of the time-dependent Ginzburg-Landau theory. From the theory of complex functions it is known that the analytical continuation of a function $f(z)$ is uniquely determined if $f(z)$ is known at an infinite number of points z_n , which form a sequence with *one*

accumulation point. However, in our case there are *two* accumulation points $z_n = i\Omega_n \rightarrow +i\infty$ and $z_n = i\Omega_n \rightarrow -i\infty$, respectively. Therefore there exist two analytical continuations. This implies that $\chi(\mathbf{K}, z)$ is analytic in the upper complex half plane $\text{Im}(z) > 0$ and in the lower complex half plane $\text{Im}(z) < 0$, but not on the real axis $\text{Im}(z) = 0$.

The formula (17) is not restricted to the strong-coupling limit. Since Eq. (17) can be interpreted as a Taylor expansion of $[\chi(\mathbf{K}, z)]^{-1}$ with respect to z and \mathbf{K}^2 up to first order, it is valid also for general couplings v if z and \mathbf{K} are sufficiently small. [The Thouless criterion (7) requires the zeroth-order term to be zero.] Thus the parameters d and c can be determined by comparing Eq. (17) with the numerical result of $[\chi(\mathbf{K}, z)]^{-1}$ for infinitesimal small z and \mathbf{K} . Since for $z = i\Omega_n = 0$ it is $[\chi(\mathbf{K}, 0)]^{-1} = [\Gamma(\mathbf{K}, 0)]^{-1}$, the coefficient c can be determined directly from the vertex function. Thus we obtain a real c with a high numerical accuracy. The symmetry equation $\Gamma(\mathbf{K}, -\Omega_n) = [\Gamma(\mathbf{K}, \Omega_n)]^*$ relates the two analytical continuations to each other, $\chi(\mathbf{K}, z^*) = [\chi(\mathbf{K}, z)]^*$. Therefore in Eq. (17) the parameter $d = d' \pm id''$ is complex for $\text{Im}(z) \gtrless 0$, respectively, with real part d' and imaginary part d'' . Therefore, in order to obtain d we determine the analytical continuation of $[\chi(0, z)]^{-1}$ in the upper complex half plane $\text{Im}(z) > 0$. To do this we approximate $[\chi(0, z)]^{-1}$ by a polynomial $d_0 \hbar z + d_2 (\hbar z)^2 + \dots + d_l (\hbar z)^l$ of degree l and determine the coefficients d_0, d_2, \dots, d_l by requiring $[\chi(0, z_n)]^{-1} = [\Gamma(0, \Omega_n)]^{-1}$ at $z_n = i\Omega_n = i2\pi n k_B T / \hbar$ with $n = 0, 1, 2, \dots, N_l$, where N_l must be chosen appropriately. The procedure works well if d and the other coefficients converge to some limiting values for increasing l . We find a quite good convergence for the real part d' if we use only odd powers of z . On the other hand for d'' we need odd and even powers of z . Since in the latter case the convergence is much slower, the accuracy of our numerical values for d'' is not so good as for d' . We obtain d' and d'' with numerical inaccuracies of about 0.3% and 3% relative to $|d| = [d'^2 + d''^2]^{1/2}$, respectively.

Now, by comparing (14) with (17) substituting $i\Omega_n \rightarrow z$ we obtain Z and $2m^*$ from d and c . Since the renormalization factor Z is canceled in physical quantities (at least for strong couplings, see Ref. 1, Sec. 3B), and therefore it cannot be observed, we restrict our considerations to the complex effective boson mass

$$2m^* = m(d' + id'')/c. \quad (18)$$

Such a formula for the effective mass has been found also in the Ginzburg-Landau theory.⁴ In Figs. 5 and 6 we present the numerical results of the real and the imaginary part of $2m^*$ as functions of the coupling strength v , respectively. For strong-coupling $v \gtrsim 1$ the real part decreases with increasing coupling strength v , while the imaginary part is nearly zero. The weak repulsive interaction between the bosons described by the scattering length $a_B = 2a_F$ (Ref. 1) causes a real part $\text{Re}(2m^*)$ somewhat larger than $2m$, which up to first order is given by (15). This fact is expected because for strong coupling $v \gtrsim 1$ the system behaves like a weakly interacting Bose

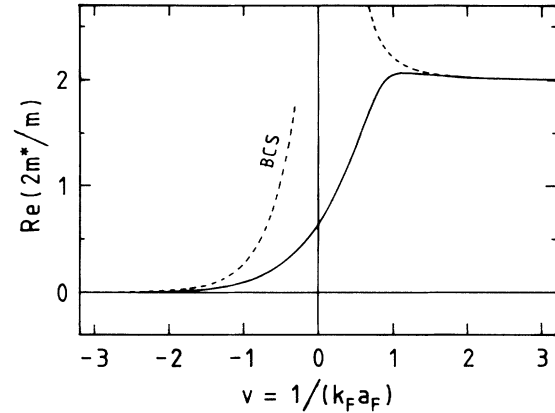


FIG. 5. The real part of the effective boson mass $2m^*$ vs the dimensionless coupling strength v . The full line represents our numerical result. The left-hand dashed line corresponds to the BCS theory, (19). The right-hand dashed line represents our asymptotical strong-coupling result (15).

gas (see Ref. 2, Sec. 28). In Fig. 5 one clearly sees that for $v \gtrsim 2$ the numerical result of $2m^*$ (full line) converges quite well to the asymptotical formula (15) (right-hand dashed line). Contrary to $T_c(v)$ in Fig. 1 in this case the numerical result is very accurate because $2m^*$ does not depend explicitly on the fermion density n_F . For intermediate and weak coupling $v \lesssim 1$ part of the pairs is broken up into free fermions. This causes a finite lifetime of the bosons, which is reflected by a positive imaginary part of the effective mass in Fig. 6. (The small negative imaginary part for values of v between 1.1 and 1.7 would cause an instability. Presumably it is an artifact of our approximate analytical continuation described above.) The interaction of the bosons with the free fermions causes a decrease of the real part $\text{Re}(2m^*)$ with decreasing coupling strength v , as it can be seen in Fig. 5. Thus near $v \approx 1$ the real part has a maximum, which is, however, rather tiny. At $v = 0$ real and imaginary part are nearly equal and for $v < 0$ the imaginary part becomes dominant, while for $v > 0$ the real part is dominant. Finally, for weak coupling $v \lesssim -1$ the imaginary part is much

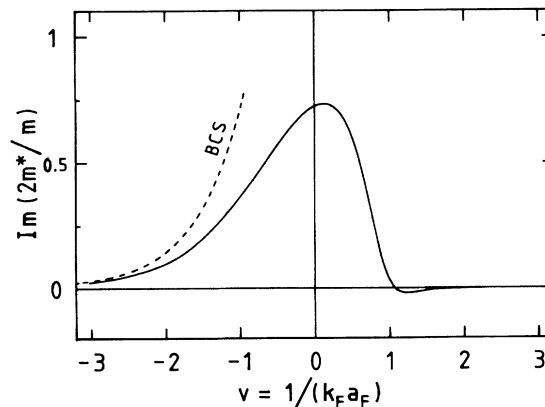


FIG. 6. The imaginary part of the effective boson mass $2m^*$ vs the dimensionless coupling strength v . The full line represents our numerical result. The left-hand dashed line corresponds to the BCS theory, (20). The negative part near $v \approx 1.3$, which would indicate an instability of the system, is presumably a numerical artifact.

larger than the real part, which means that the system is overdamped. In the weak-coupling limit the effective mass $2m^*$ can be calculated asymptotically. In this limit we obtain

$$\text{Re}(2m^*) = m \frac{3\pi^2}{7\xi(3)} \left[\frac{k_B T_c}{\epsilon_F} \right]^2 [3 - v(\pi/2)], \quad (19)$$

$$\text{Im}(2m^*) = m \frac{3\pi^2}{7\xi(3)} \frac{k_B T_c}{\epsilon_F} \frac{\pi}{2}, \quad (20)$$

respectively, where $k_B T_c$ is given by (10). These asymptotic results are shown as the left-hand dashed lines in Figs. 5 and 6 and are in accordance with our numerical results (full lines). We have observed that the numerical accuracy of the full lines becomes somewhat worse for weak couplings $v \lesssim -1$.

The results (19) and (20) agree with the conventional time-dependent Ginzburg-Landau theory of a BCS superconductor.^{11,12} We have obtained the correct expressions for the relaxation time τ_0 and the coherence length ξ ,¹³ which give $\tau_0/\xi^2 = \text{Im}(2m^*)/2\hbar$. To obtain the correct values of the real parts (19) and d' it is crucial that in the integrals the density of states $N(\epsilon)$ is *not* replaced by the constant value $N(\epsilon_F)$ at the Fermi energy ϵ_F . If one would use $N(\epsilon_F)$ the factor $[3 - v(\pi/2)]$ in (19) would be replaced by 1. However, c and the imaginary parts d'' and (20) are insensitive with respect to that.

Within the Ginzburg-Landau theory of the crossover scenario the effective boson mass $2m^*$ has been investigated previously by Zwerger⁴ for $d=2$. There a real effective boson mass has been found, which increases monotonically with increasing coupling strength and looks similar to our Fig. 5. However, a direct comparison of this result for $d=2$ with the result for $d=3$ is not reasonable.

The Ginzburg-Landau theory of the crossover scenario has been extended to a *time-dependent* Ginzburg-Landau theory by Sá de Melo, Randeria, and Engelbrecht.⁸ They derived the time-dependent Ginzburg-Landau equation

$$di\hbar \frac{\partial \Delta(\mathbf{x}, t)}{\partial t} = \left[-c \frac{\hbar^2}{2m} \nabla^2 + a + b |\Delta(\mathbf{x}, t)|^2 \right] \Delta(\mathbf{x}, t), \quad (21)$$

where $\Delta(\mathbf{x}, t)$ is the order parameter, and obtained explicit formulas for the coefficients a , b , c , and $d = d' + id''$. These results can be compared with our coefficients d and c for the following reason. The fact that $\chi(\mathbf{K}, z)$ is a susceptibility implies the linear response equation $\Delta(\mathbf{K}, z) = \chi(\mathbf{K}, z) h(\mathbf{K}, z)$, where h is the conjugate field of Δ . Since in a superfluid system the conjugate field $h(\mathbf{K}, z)$ is zero, this equation becomes

$$[\chi(\mathbf{K}, z)]^{-1} \Delta(\mathbf{K}, z) = 0. \quad (22)$$

Thus inserting (17) and performing a Fourier back transformation we obtain the time-dependent Ginzburg-Landau equation (21) with $a=0$ at $T=T_c$ and the last term neglected in the linear response approximation.

The theory of Sá de Melo, Randeria, and Engelbrecht⁸ includes the interaction between the *condensed* bosons

and thus yields $a_B = 2a_F$ according to our result.¹ However, the repulsive interaction between the *noncondensed* bosons is missing, which is a typical property of *mean-field* Ginzburg-Landau theories. Hence, this theory does not yield the first-order correction terms of c and d in the strong-coupling limit, which correspond to the first-order correction of the effective boson mass (15). On the other hand in the weak-coupling limit our asymptotic formulas (19) and (20) must coincide with the corresponding results of Ref. 8 because in this limit both theories are equivalent (see Ref. 1). However, while we find agreement for d'' , the explicit result of d' in Ref. 8 differs from our result because in the integrals of Ref. 8 the density of states $N(\epsilon)$ was replaced by the constant value $N(\epsilon_F)$ at the Fermi energy, which gives an incorrect result (see above). Furthermore, the value of c in Ref. 8 is larger by a factor 9 than our result, which is presumably due to a calculational error. In the crossover region Sá de Melo, Randeria, and Engelbrecht⁸ have found an algebraic singularity of the coefficient d and the effective mass $2m^*$ at an interaction strength v_0 , which corresponds to the chemical potential $\mu=0$ (see Fig. 2). While for $v > v_0$ (where $\mu < 0$) the imaginary parts are $d''=0$ and $\text{Im}(2m^*)=0$, for $v < v_0$ (where $\mu > 0$) these imaginary parts are nonzero. However, this singularity is an artifact of the approximation made in Ref. 8. While the same singularity can be found in our theory if the free-fermion Green's function (8) is inserted into (4) and (2), it is not present in our *self-consistent* theory. This fact is confirmed by our numerical results of the effective boson mass $2m^*$ because in Figs. 5 and 6 the full lines are *smooth* for couplings near $v_0 \approx 0.5$.

IV. CONCLUSIONS

The numerical analysis has shown that the self-consistency is essential in the theory of the crossover from BCS superconductivity to Bose-Einstein condensation. Since our theory includes the interaction between the *condensed* and *noncondensed* fermion pairs the superfluid transition temperature $T_c(v)$ is a monotonically growing function of the coupling strength v *without* a maximum in the crossover region. (This result was found in $d=3$ dimensions.) The bound fermion pairs are represented as a power-law tail $\sim k^{-4}$ in the fermion occupation number $n(k)$ for momenta $\hbar k$ in the interval $\max(k_F, a_F^{-1}) \ll k \ll r_0^{-1}$, where r_0 is the effective range of the interaction. While for strong coupling $v \gtrsim 1$ the system behaves like a weakly interacting Bose gas, in the intermediate and weak-coupling range $v \lesssim 1$ the fermion pairs are bosonic quasiparticles with a short lifetime expressed by an imaginary part of the effective mass $2m^*$. The self-consistency guarantees that all quantities are smooth functions of v , in contrast to the results of Ref. 8.

Our numerical procedure is a powerful method for solving the self-consistent equations, which is not restricted to the superfluid transition at $T=T_c$ but can be applied for arbitrary temperatures T . For future investigations of special interest are thermodynamic quantities like the specific heat $C_v(T)$ and the compressibility $\kappa_T(T)$

at given values of the invariant coupling strength $v = 1/k_F a_F$. Furthermore the microscopic functions \mathcal{G} and Γ can be used to derive the linearized hydrodynamic equations and to determine transport coefficients like the thermal conductivity $\lambda(T)$ and the shear viscosity $\eta(T)$. This must be done by an analytical continuation analogously, as we have shown above, because hydrodynamic equations represent a direct generalization of the time-dependent Ginzburg-Landau theory. The resulting physical quantities could then be used for a comparison with experiments.

ACKNOWLEDGMENT

I wish to thank Professor W. Zwerger for discussions and for comments on the manuscript.

APPENDIX

Here we briefly describe our numerical Fourier transformation procedure, which we have used for calculating \mathcal{G} and Γ . The numerical work can be reduced considerably by exploiting the rotational symmetry of the system, which implies that the functions \mathcal{G}, Σ and Γ, \mathcal{M} depend only on the absolute values k, K , and r of \mathbf{k}, \mathbf{K} , and \mathbf{x} , respectively. Thus the Fourier transformation formulas (5) and (6) become effectively two dimensional. We need a one-dimensional *continuous* Fourier transformation for transforming the functions in this variables $k \leftrightarrow r$ or $K \leftrightarrow r$ and $\tau \rightarrow \omega_n$ or $\tau \rightarrow \Omega_n$, respectively. Furthermore, we need a *discrete* Fourier transformation for transforming the functions in the variables $\omega_n \rightarrow \tau$ or $\Omega_n \rightarrow \tau$.

For simplicity we consider first the one-dimensional continuous Fourier transformation

$$f(p) = \int_{-\infty}^{+\infty} dx e^{-ipx} f(x). \tag{A1}$$

We assume that the values of the function $f_m = f(x_m)$ are known at the discrete points

$$x_m = \gamma^{-1} sh(\gamma \Delta x m), \tag{A2}$$

where $m = 0, \pm 1, \pm 2, \dots, \pm N$. This choice of discrete points automatically yields a good resolution on a logarithmic scale, ranging from the small value Δx up to the very large value $X = \pm(2\gamma)^{-1} \exp(\gamma \Delta x N)$. A conventional fast-Fourier-transformation procedure¹⁴ cannot be used here because the points (A2) are not equidistant. Therefore, we have to construct a special "slow Fourier transformation," which is suitable for our problem. To do this we approximate the function $f(x)$ for continuous values of x in between the points x_m by cubic spline-interpolation polynomials¹⁴ and then evaluate the Fourier integral (A1) exactly. Thus, once we have determined the coefficients of the spline polynomials, the Fourier integral (A1) has been reduced to a sum over m , which can be evaluated easily numerically. This procedure works well

for intermediate and large values of p . Since the Fourier integral (A1) is evaluated *exactly* in the intervals in between the discrete points x_m , the oscillating factor e^{-ipx} causes no difficulties even for large p . However, for very small p the procedure breaks down numerically because it contains terms of the orders p^{-4}, p^{-3}, p^{-2} , and p^{-1} , which *must* cancel for $p \rightarrow 0$. Therefore, for small p we need a second numerical procedure. In the latter case we assume that e^{-ipx} oscillates at most once in between two adjacent points x_m . Then the whole integrand $e^{-ipx} f(x)$ may be approximated by spline-interpolation polynomials so that the integral can be evaluated exactly. Thus the Fourier integral (A1) is reduced again to a sum over m , which can be evaluated numerically. Finally, the two numerical procedures must be combined to obtain a high-quality Fourier transformation. To do this we choose an optimized smooth cutoff function $b(\xi)$ and split $f(x)$ into two functions $f_p^{(1)}(x) = [1 - b(px)]f(x)$ and $f_p^{(2)}(x) = b(px)f(x)$, which are transformed by the first and the second numerical procedure, respectively.

Our procedure can be generalized to a *discrete* Fourier transformation

$$f(\tau) = \sum_{\omega_n} e^{-i\omega_n \tau} f(\omega_n). \tag{A3}$$

Here we take the values $f_m = f(\omega_n^{(m)})$ only at those Matsubara frequencies $\omega_n^{(m)}$ into account, which lie closest to points x_m given by a formula of type (A2). For all other ω_n in between we approximate $f(\omega_n)$ or $e^{-i\omega_n \tau} f(\omega_n)$ by spline-interpolation polynomials. Then we proceed in precisely the same way as in the continuous case. Inserting the spline polynomials we can evaluate the sum (A3) over the Matsubara frequencies exactly. Thus a sum over m containing the spline coefficients remains, which can be evaluated numerically. It turns out that the zero temperature limit $T \rightarrow 0$, which corresponds to the limit *discrete* \rightarrow *continuous* is no problem for our transformation procedure because of the use of the spline interpolation.

We have tested our numerical Fourier-transformation procedures very carefully. It turns out that 100 points x_m or $\omega_n^{(m)}$ are sufficient to transform a function $f(x)$ or $f(\omega_n)$, which has a nontrivial structure on a *logarithmic* scale over *six* or even *ten* decades.

Now we turn back to the Green's function \mathcal{G} and the vertex function Γ . Since they depend on two variables we need 100×100 points defined by formulas similar to (A2) to discretize (k, ω_n) , (K, Ω_n) , and (r, τ) , respectively. We perform the Fourier transformation first in one variable and then in the second variable. Thereby it is important to subtract the singularities of the functions \mathcal{G} and Γ carefully, as we have described in Sec. II. Thus, using Eqs. (1)–(4) and the Fourier transformation (FT) we obtain the following iteration procedure to determine \mathcal{G} and Γ :

$$\begin{aligned} \mathcal{G}(k, \omega_n) &\xrightarrow{\text{FT}} \mathcal{G}(k, \tau) \xrightarrow{\text{FT}} \mathcal{G}(r, \tau) \xrightarrow{(4)} \mathcal{M}(r, \tau) \xrightarrow{\text{FT}} \mathcal{M}(K, \tau) \xrightarrow{\text{FT}} \mathcal{M}(K, \Omega_n) \\ &\xrightarrow{(3)} \Gamma(K, \Omega_n) \xrightarrow{\text{FT}} \Gamma(K, \tau) \xrightarrow{\text{FT}} \Gamma(r, \tau) \xrightarrow{(2)} \Sigma(r, \tau) \xrightarrow{\text{FT}} \Sigma(k, \tau) \xrightarrow{\text{FT}} \Sigma(k, \omega_n) \xrightarrow{(1)} \mathcal{G}(k, \omega_n). \end{aligned}$$

Fortunately, in repeating the iteration procedure no numerical instabilities have occurred. We have found that 13 iteration steps are sufficient to achieve a convergence better than 0.1%, which is better than the numerical accuracy. Since we have used only 100×100 points for discretizing the functions, the numerical work is comparatively moderate. Thus, a high performance computer is not necessary.

¹R. Haussmann, *Z. Phys. B* **91**, 291 (1993).

²A. L. Fetter and J. D. Walecka, *Quantum Theory of Many-Particle Systems* (McGraw-Hill, New York, 1971).

³A. A. Abrikosov, L. P. Gorkov, and I. E. Dzyaloshinskii, *Methods of Quantum-Field Theory in Statistical Physics* (Dover, New York, 1963).

⁴W. Zwerger, in *Proceedings on the Conference on Path Integrals from meV to MeV, Tutzing, Germany, 1992*, edited by A. Inomata (World Scientific, Singapore, in press).

⁵P. Nozières and S. Schmitt-Rink, *J. Low Temp. Phys.* **59**, 195 (1985).

⁶M. Drechsler and W. Zwerger, *Ann. Phys.* **1**, 15 (1992).

⁷S. Stintzing and W. Zwerger (private communication).

⁸C. A. R. Sá de Melo, M. Randeria, and J. R. Engelbrecht, *Phys. Rev. Lett.* **71**, 3202 (1993).

⁹P. Ring and P. Schuck, *The Nuclear Many-Body Problem* (Springer, Berlin, 1980), Chap. 5.6, p. 203.

¹⁰D. J. Thouless, *Ann. Phys. (N.Y.)* **10**, 553 (1960).

¹¹A. Schmid, *Phys. Kondens. Mater.* **5**, 302 (1966).

¹²E. Abrahams and T. Tsuneto, *Phys. Rev.* **152**, 416 (1966).

¹³M. Tinkham, *Introduction to Superconductivity* (McGraw-Hill, New York, 1975).

¹⁴J. Stoer, *Einführung in die Numerische Mathematik 1* (Springer, Berlin, 1983).